Journal of Geodesy (2019) 93:877–888
https://doi.org/10.1007/s00190-018-1210-7

ORIGINAL ARTICLE

Helmert-VCE-aided fast-WTLS approach for global ionospheric VTEC modelling using data from GNSS, satellite altimetry and radio occultation

Andong Hu[1] · Zishen Li[3] · Brett Carter[1] · Suqin Wu[1] · Xiaoming Wang[3] · Robert Norman[1] · Kefei Zhang[1,2]

Received: 16 November 2017 / Accepted: 21 October 2018 / Published online: 14 November 2018

Abstract
Vertical total electron content (VTEC) global ionospheric maps (GIM) are commonly used to correct the ionospheric delay of global navigation satellite system (GNSS) signals for single-frequency positioning and other ionospheric studies. The measurements observed by inhomogeneously distributed ground reference stations are the only data used to generate the GIMs. Thus the accuracy of the GIMs over ocean and polar regions is relatively poor due to the lack of measurements over these regions. In this study, space-borne VTECs obtained from ocean-altimetry and GNSS radio occultation measurements are incorporated into the modelling process. Since the three types of VTEC data have different qualities, the weight for each type of data is determined using the Helmert-variance component estimation (Helmert-VCE) method. In addition, unlike the traditional weighted least squares (WLS) estimation method in which the design matrix of observation equations is fixed, in this study, the design matrix, especially those elements in design matrix that are derived from the coordinates of either tangent point or ionospheric pierce point, are considered to be inaccurate. Thus they are adjusted together with the unknown coefficient parameters of the fitting model using the fast-weighted total least squares (fast-WTLS) technique. The proposed approach, named Helmert-WTLS, was tested using the data in the period of day of year (DOY) 217–224, 2016 and validated using GIMs produced by the research team for ionosphere and precise positioning based on BDS/GNSS (GIPP) at the Academy of Opto-Electronics, Chinese Academy of Sciences (CAS). Comparison results showed that the GIMs (with a 2 h temporal resolution) generated using the new approach can improve the determination of ionospheric TEC by 0.28 TEC units (TECU) over those from the Helmert-VCE-aided WLS approach (w.r.t CAS references, respectively) and by 1.61 TECU better than those from WLS, in terms of the mean of all root-mean-squares errors of all 2 h time slots in the 8-day testing period. In addition, in comparison with out-of-sample Jason-3 observations, results from the proposed method also outperformed Helmert-VCE-aided WLS, CAS and CODE models by 1.5, 2.4 and 2.4 TECU, respectively.

Keywords Global navigation satellite system (GNSS) · Radio occultation · Satellite altimetry · VTEC · GIM · WTLS · Helmert-VCE

1 Introduction

The ionosphere is a region of the Earth's upper atmosphere in the altitude range of 60–1500 km above the mean sea level, where free electrons interfere with the propagation of electromagnetic waves, such as GPS signals (Hajj et al. 1994; Wang et al. 2016). The ionospheric delay is proportional to the total electron content (TEC) along the ray path and inversely proportional to the frequency of the signal squared. It is one of the major errors in GNSS measurements, which affects the performance of GNSS applications such as single-frequency positioning. If this delay can be accurately estimated, the ionospheric error in GNSS measurements can be corrected

✉ Andong Hu
andong.hu@rmit.edu.au

✉ Kefei Zhang
Kefei.Zhang@rmit.edu.au

1 SPACE Research Centre, School of Sciences, RMIT University, Melbourne 3000, Australia

2 School of Environmental Science and Spatial Informatics, China University of Mining and Technology, Xuzhou 221116, China

3 Academy of Opto-Electronics, Chinese Academy of Sciences, Beijing 100094, China

or mitigated. Since the ionosphere is a dispersive medium, the ionospheric delay can be largely mitigated using the differential approach—a linear ionosphere-free combination of simultaneous dual-frequency GNSS measurements. However, for single-frequency measurements, the ionospheric delay cannot be mitigated through the differential approach. In this case, an ionospheric model can be used to correct the ionospheric delay at the user's location. The ionospheric model, which can be global-scale or regional-scale depending on the coverage of the data, can be derived from a network of GNSS reference stations where dual-frequency receivers are deployed. The vertical TEC (VTEC) values over all the network stations are often used to establish a VTEC model for the region covered.

Several types of global empirical VTEC models have been developed, e.g. the Global Assimilative Ionospheric Model (GAIM) (Scherliess et al. 2004; Schunk et al. 2004), and empirical models such as NeQuick (Hochegger et al. 2000; Radicella and Leitinger 2001) and the International Reference Ionosphere (IRI) (Bilitza 1997, 2001; Bilitza et al. 1990; Bilitza and Reinisch 2008). In addition, several different global ionosphere maps (GIMs) are produced by a number of IGS data processing centres, including European Space Agency (ESA), the EMRG from Canadian Geodetic Survey (CGS), Centre for Orbit Determination in Europe (CODE), etc. All of these GIMs are near real-time ionospheric products using a similar approach (i.e. spherical harmonic (SH) models with a 2 h temporal resolution). Detailed comparison among the current GIMs can be found in Hernández Pajares et al. (2016).

Traditionally, TEC data used for producing GIMs are obtained from ground-based GNSS measurements collected at global IGS stations. In a 2-h period, the number of measurements can reach one million, which is regarded to be sufficient for generating a high-accuracy GIM (Hernández-Pajares et al. 1999, 2009; Mannucci et al. 1998]. Li et al. (2015) estimated GIMs by an innovative approach—spherical harmonic plus generalised Trigonometric Series functions (SHPTS) and the data from the BeiDou-2 system were also used in the modelling. However, due to the lack (or low number) of IGS stations in some regions, especially over the oceans, the GIMs produced may not perform well across the entire globe.

In order to improve the performance of GIMs, Todorova et al. (2008) established another GIM by incorporating VTECs derived from GNSS measurements with satellite altimetry (e.g. Jason-1) measurements mainly for compensating insufficient data over the oceans. The performance of the GIMs showed significant improvements, but the inhomogeneous distribution of the satellite altimetry data over the oceans still limited the model's performance. To overcome this problem, Alizadeh et al. (2011) took into consideration an additional data source—VTECs retrieved from radio occultation (RO) of the Constellation Observing System for Meteorology Ionosphere and Climate (COSMIC/FORMOSAT-3) satellites into global ionospheric modelling and the accuracy of the VTEC GIMs over the ocean regions were further improved. The combined GIMs of VTEC show a maximum difference of 1.3–1.7 TECU with respect to the GNSS-only GIMs in the whole day (Alizadeh et al. 2011). Dettmering et al. (2011) computed regional models of VTEC based on the IRI 2007 and observations from ground GNSS stations, radio occultation data from low earth orbiters, dual-frequency radar altimetry measurements and data obtained from Very Long Baseline Interferometry. Reliable VTEC maps with high resolution and accuracies better than 2 TECU can be achieved by using this method.

When the VTEC data used in the least squares estimation for the optimal coefficient estimates of the ionospheric model have different precisions or qualities, the use of appropriate weights plays an important role in getting good estimates. Therefore, instead of using the a priori variance (or covariance) of the observations to determine the weights, Chen et al. (2015) applied a Helmert-variance component estimation (VCE) method to estimate the variance of each type of observations, and the results showed further improvement to the GIMs.

In addition, each element in the design matrix of the observation equations is usually a fixed value derived from the approximate coordinates of the ionospheric pierce point (IPP) for each of the VTECs derived from ground-based GNSS and Jason observations. However, for each RO-derived VTEC, the coordinates for the tangent point (similar to the IPP for a GNSS observation) of the RO event change during the event, which can last 1–2 min. Thus, the tangent point coordinates are no longer fixed values and can move up to 10° in the geomagnetic coordinate frame. This means that neglecting the uncertainty in the elements of the design matrix may not be appropriate. In this study, the fast-weighted total least squares (fast-WTLS) method (Golub and Van Loan 1980; Schaffrin and Wieser 2008; Shen et al. 2011) was adopted instead of using the conventional least squares estimation. In addition, the uncertainty of the elements in the design matrix was also taken into account in this approach. Moreover, for reducing the large computational load of the model estimation process, the sequential technique was also used rather than the conventional batch processing approach.

The outline of the paper is as follows. In Sect. 2, three sources of VTEC data used to generate the GIMs for this study are briefly introduced, together with the detailed methodology and procedure of the traditional GIM modelling. Section 3 elaborates the Helmert-VCE-aided fast-WTLS (Helmert-WTLS) method. This is followed by a performance assessment of the GIMs generated using the above three sources of data as well as various other GIM

modelling approaches presented in Sect. 4. Section 5 outlines conclusions.

2 Data sources

Global VTEC information can be obtained using a number of different techniques. In this study, VTECs obtained from IGS, COSMIC and Jason-3 data (denoted as ground-based GNSS data, GNSS-RO data and satellite altimetry data, respectively) were used to construct GIMs. It should be noted that TOPEX/Poseidon data have a +3 TECu bias in comparison with the GIM (Azpilicueta and Brunini 2009; Imel 1994). TOPEX/Poseidon was succeeded by Jason-1, Jason-2 and later Jason-3 (Dumont et al. 2016). The details for each of the three types of data used in this study are presented below.

2.1 IGS data

The absolute slant TEC (STEC) of a GNSS signal can be retrieved from dual-frequency observations collected at ground GNSS stations as follows:

$$\mathrm{STEC} = \frac{f_1^2 f_2^2}{40.28\left(f_1^2 - f_2^2\right)}\left(P_2 - P_1 + b_k + b^{\delta}\right) \tag{1}$$

where P_1 and P_2 are the simultaneous pseudo-range observations on the two frequencies f_1 and f_2, respectively; b_k and b^{δ} are the differential code biases (DCBs) of the satellite and receiver, respectively (Ciraolo et al. 2007; Mannucci et al. 1998).

DCBs determination is essential for the absolute TEC derivation, and in this study, the DCBs were precisely estimated using IGGDCB method proposed by Li et al. (2012). It was demonstrated by Li et al. (2012) that the accuracies of the IGGDCB-based DCB estimates perform at the level of about 0.13 and 0.10 ns during periods of high (2001) and low (2009) solar activities, respectively. Different from the traditional method, IGGDCB determines DCBs in two steps: the first step is to individually estimate the sum of satellite and receiver DCBs at each station using the regional ionospheric model and the second step is to separate the satellite and receiver DCBs by introducing a zero-mean reference imposed on the DCBs of all the satellites. The standard derivation of the DCBs can be obtained during step two as well.

The VTEC used in the GIM modelling are obtained from the STEC using a mapping function which is under spherical symmetry assumption. The intersection of each signal path and the single ionospheric layer (assumed to be, e.g. 350 km height) is called the signal's IPP. The most commonly used trigonometric projection function is:

$$\mathrm{VTEC} = \mathrm{STEC} \cdot \cos z' \tag{2}$$

where z' is the zenith angle of the satellite at the IPP.

Furthermore, DCBs and z' were also used to determine the weight of each GNSS signal/observation in the modelling process as:

$$\sigma^0_{\mathrm{IGS}} = \frac{f_1^2 f_2^2}{40.28\left(f_1^2 - f_2^2\right)} * \cos z' * \sqrt{\Delta b_k^2 + \Delta b^{\delta 2}}, \tag{3}$$

where Δb_k and Δb^{δ} are the standard deviation of DCBs of the satellite and receiver, respectively, and Eq. (3) can be derived from Eqs. (1) and (2).

2.2 COSMIC data

The Constellation Observing System for Meteorology Ionosphere and Climate (COSMIC/FORMOSAT-3) is a six-satellite radio occultation mission that was launched in mid-April, 2006 (Schreiner et al. 2007). The COSMIC satellites orbit at approximately 850 km altitude, allowing them to measure the electron density under 850 km using RO. COSMIC's designed mission lifecycle was 2006–2010, and it was estimated that approximately 2000 (ionospheric) RO events could be measured every day during that period (Anthes et al. 2008; Schreiner et al. 2007). Some COSMIC satellites are still collecting RO data; however, currently it can only provide about 400–500 global (ionospheric) RO events per day. Its RO measurements have high accuracy, high vertical resolution and global coverage (Alizadeh et al. 2011). The "ionprf" product from the COSMIC Data Analysis and Archive Centre (CDAAC) provides the VTEC at the position of the maximum electron density of every RO event. The equation is (Sokolovskiy and Rocken 2006):

$$\mathrm{VTEC\_RO} = \mathrm{VTEC0} + \mathrm{VTEC1} \tag{4}$$

where VTEC0 and VTEC1 are the VTEC under and above the LEO satellite orbit, respectively. VTEC0 is obtained by integrating the derived electron density along the path of all the tangent points, and VTEC1 is obtained from an extrapolation of a model which can be an empirical/physical ionospheric model (e.g. Chapman-α, exponential model (Sokolovskiy and Rocken 2006), even though the extrapolated VTEC is unlikely to be as accurate as observed ones.

In this study, the weight of each RO observation is determined based on its maximum altitude of the satellite orbit (i.e. the boundary between the observed and the extrapolated ranges) because the VTEC below the orbit of the satellite is measurable (i.e. $\sigma^0_{\mathrm{RO}} = 1/(0.6*(2000 - h_{\max}) + 1*h_{\max})$,

where hmax equates to the maximum altitude of the Ne profile and they were extracted from the ionPrf file directly.

2.3 Jason-3 data

The Jason-3 mission is one of the latest altimetry satellite missions and can provide global coverage VTEC data, mostly over the ocean. The Jason-3 satellite is mainly used to measure the variation of the sea level and to obtain fundamental information for tides. With a 66° orbital inclination and a 1336 km altitude, the trajectories of the satellite cover the latitudinal range from 66° N to 66° S; the polar regions are not measured. There are two bands used in Jason-3 measurements: Ku-band (main band, frequency is 13.575 GHz) and a C-band (auxiliary band, frequency is 5.3 GHz). The VTEC is mostly derived from Ku-band measurements (Dumont et al. 2016).

VTEC can be calculated by

$$\mathrm{VTEC} = -\frac{\mathrm{d}R \cdot f^2}{40.28}, \tag{5}$$

where f is the frequency of the Ku-band and dR is the Ku-band ionospheric range correction provided by the output of Jason-3 directly. Due to the 1336 km altitude of the satellite, the VTEC above this altitude is neglected in this study.

The onboard radar altimeters can directly access the differential ionospheric delay of the transmitted signals which can be used as an ionospheric correction dR. The error or uncertainty is usually no larger than 2–3 TECu. Each Jason-3 measurement is considered having equal quality in this study; their initial sigma $\sigma^0_{\mathrm{Jason}}$ was set to 3.

3 GIM generation using Helmert-VCE-aided fast-WTLS approach

In this study, in addition to the Helmert-VCE (Chen et al. 2015), fast-WTLS is also applied in GIM establishment in order to minimise the uncertainty of the design matrix from the uncertainties of the tangent points of the events. The detailed procedures of the purposed approach are presented below.

3.1 Spherical harmonics (SH)

The most commonly used global ionospheric model is a SH function. For example, a SH function of 15×15 order is adopted by most IAACs to generate GIMs:

$$\mathrm{VTEC}(\beta, s) = \sum_{n=0}^{N} \sum_{m=0}^{n} \tilde{P}_{nm}(\sin\beta)\left(\tilde{C}_{nm}\cos(ms) + \tilde{S}_{nm}\sin(ms)\right) \tag{6}$$

where β and s are the latitude and longitude of the IPP under a sun-fixed geomagnetic coordinate frame; N is the maximum degree of the function expansion; $\tilde{P}_{nm}(\sin\beta)$ is the normalised Legendre function of degree n and order m; and $\tilde{C}_{nm}$ and $\tilde{S}_{nm}$ are the unknown coefficients of the SH model.

The temporal resolution of the model is 2 h, and the spatial intervals of the global grids in the latitudinal and longitudinal directions are 2.5° and 5°, respectively.

3.2 Weighted least squares (WLS)

The WLS is a traditional method that is based upon spherical harmonics. It can be formulated as following:

$$x = \left(A^T P A\right)^{-1} A^T P y, \tag{7}$$

where x is the cluster of the unknown coefficients (in this study, $\tilde{C}_{nm}$ and $\tilde{S}_{nm}$), and y is the measurements of dependent variables (in this study, VTECs).

The normal equation for the traditional WLS for estimating the unknown coefficients in this study is:

$$\begin{aligned} N_{\mathrm{COMB}} &= \sigma^2_{\mathrm{GNSS}} N_{\mathrm{GNSS}} + \sigma^2_{\mathrm{ALT}} N_{\mathrm{ALT}} + \sigma^2_{\mathrm{RO}} N_{\mathrm{RO}} \\ &= \sigma^2_{\mathrm{GNSS}} \left(A^T_{\mathrm{GNSS}} P_{\mathrm{GNSS}} A_{\mathrm{GNSS}}\right) \\ &\quad + \sigma^2_{\mathrm{ALT}} \left(A^T_{\mathrm{ALT}} P_{\mathrm{ALT}} A_{\mathrm{ALT}}\right) \\ &\quad + \sigma^2_{\mathrm{RO}} \left(A^T_{\mathrm{RO}} P_{\mathrm{RO}} A_{\mathrm{RO}}\right), \end{aligned} \tag{8}$$

where N is the matrix of all the normal equations; A is the design matrix of the observational equation system; P is the weight matrix of the observations; and σ is the standard error of an observation of unit weight.

In addition, the sizes of different types of data sets are largely different, e.g. the amount of IGS data is hundreds of times larger than the other types of data. Therefore, the quantity of each type of measurements is used to determine its initial weight:

$$W^0_i = \frac{\Sigma_i}{\sqrt{\mathrm{num}_i}},$$

where i denotes the type of the data: IGS, JASON, COSMIC; $\Sigma = \{\sigma_1, \sigma_2, \ldots, \sigma_j, \ldots, \sigma_{num}\}$, and j is the index of measurements from this data source; and num is the quantity of the data.

3.3 Helmert-variance component estimation

In order to determine a set of appropriate weights for the three sources of VTECs, Chen et al. (2015) applied the Helmert-VCE method to adjust the variance factor (weight) of each type of the data. It was a recursive process starting from a

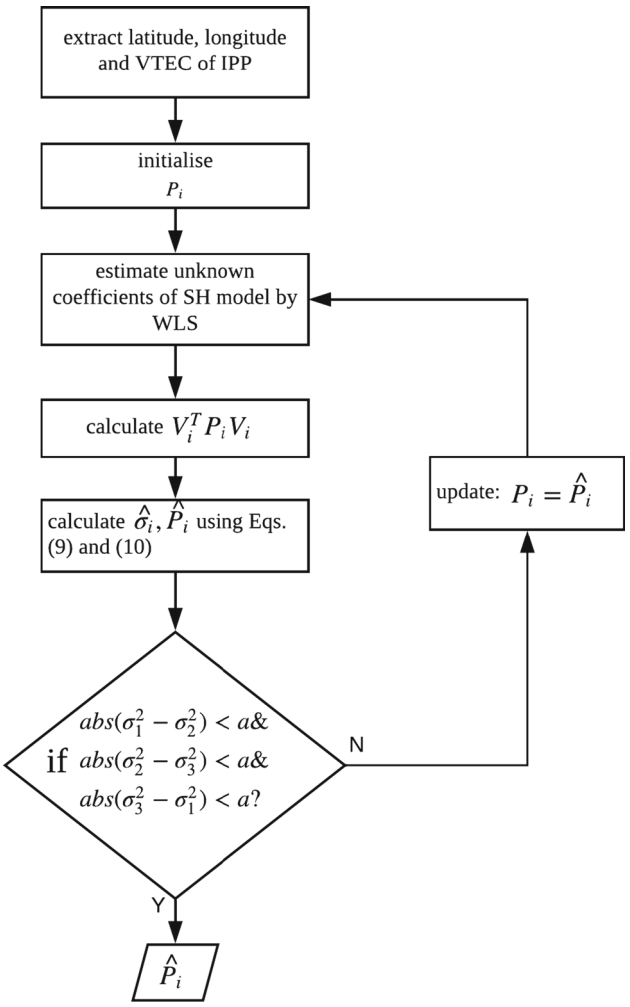

Fig. 1 Procedure of Helmert-VCE (a is a pre-set threshold and $a = 10^{-3}$ TECU^2 in this study)

set of initial a priori values, as shown in Fig. 1 in which $\hat{P}_1$, $\hat{P}_2$, and $\hat{P}_3$ denote the final weights of IGS, RO and altimetry data, respectively. In addition, "update: $A = B$" in flowchart means "to set A equal to B", and all the equations involved in the calculation have been listed in the figure.

It is noted that, theoretically, the Helmert-VCE process is very complicated and involves a considerable computational load (CL) due to high-dimensional matrices to be computed. Thus in practice simplified formulas, as expressed as below, are often used (Xu et al. 2006):

$$\hat{\sigma}_i^2 = \frac{V_i^T P_i V_i}{n_i} \tag{9}$$

$$\hat{P}_i = \frac{c}{\hat{\sigma}_i^2 P_i^{-1}} \tag{10}$$

where c can be any constant value but usually one of the $\hat{\sigma}_i^2$ values is assigned to it; the subscript i denotes the index of the data type.

3.4 Fast-WTLS

The weighted total least squares (WTLS) method is applied in this study to mitigate the error caused by the uncertainty of independent variables (e.g. linearised nonlinear functions). It differs from the traditional least squares in that the errors in the elements of the design matrix of the observational equations are also taken into account. It can be applied to both linear and nonlinear models.

The WTLS model is expressed as

$$y + e_y = (A + E_A)X, \tag{11}$$

where $y \in R^{N\times 1}$ is the vector of observations; e_y is the vector of the random noise/error of the observations; $A \in R^{N\times M}$ and E_A are the design matrix and its random error matrix, respectively; and $X \in R^{M\times 1}$ is the vector of the unknown coefficient parameters.

Specifically, in this study, y is the VTEC value as an observation; A is the coefficients $\tilde{C}_{nm}$ and $\tilde{S}_{nm}$ as expressed in Eq. (4); and N and M are the numbers of the VTEC observations and coefficients of the SH model $(l+1)^2$ (l is an assumed maximum degree of the SH model).

It is noted that P_A (i.e. the vectorisation of $\hat{E}_A$) needs to be estimated before the fast-WTLS process can be performed. P_y ($\hat{P}_{\text{IGS}}$, $\hat{P}_{\text{RO}}$, and $\hat{P}_{\text{Jason}}$) is determined by the aforementioned Helmert-VCE process. The fundamental equations for the fast-WTLS solution can be expressed as (Golub and Van Loan 1980; Schaffrin and Wieser 2008; Shen et al. 2011):

$$X^0 = \left(A^T P_y A\right)^{-1} A^T P_y y, \tag{12}$$

$$\hat{X} = X^0 + \hat{x}, \tag{13}$$

$$\hat{x} = \left(A^T Q_{VV}^{-1} A\right)^{-1} A^T Q_{VV}^{-1} W, \tag{14}$$

where $W = y - AX^0$ and:

$$Q_{VV} = K Q_{\text{vec}\left(\hat{G}\right)} K^T \tag{15}$$

and $K = \left[I_n \; -X^{0T} \otimes I_N\right]$, $K \in R^{N\times(NM+N)}$, and $Q_{\text{vec}\left(\hat{G}\right)} \in R^{(NM+N)\times(NM+N)}$,

$$\hat{G} = \begin{bmatrix} \begin{pmatrix} \hat{e}_{y_1} & \hat{E}_{A_{11}} & \cdots & \hat{E}_{A_{1M}} \\ \vdots & & \ddots & \vdots \\ \hat{e}_{y_N} & \hat{E}_{A_{N1}} & \cdots & \hat{E}_{A_{NM}} \end{pmatrix} \end{bmatrix}, \tag{16}$$

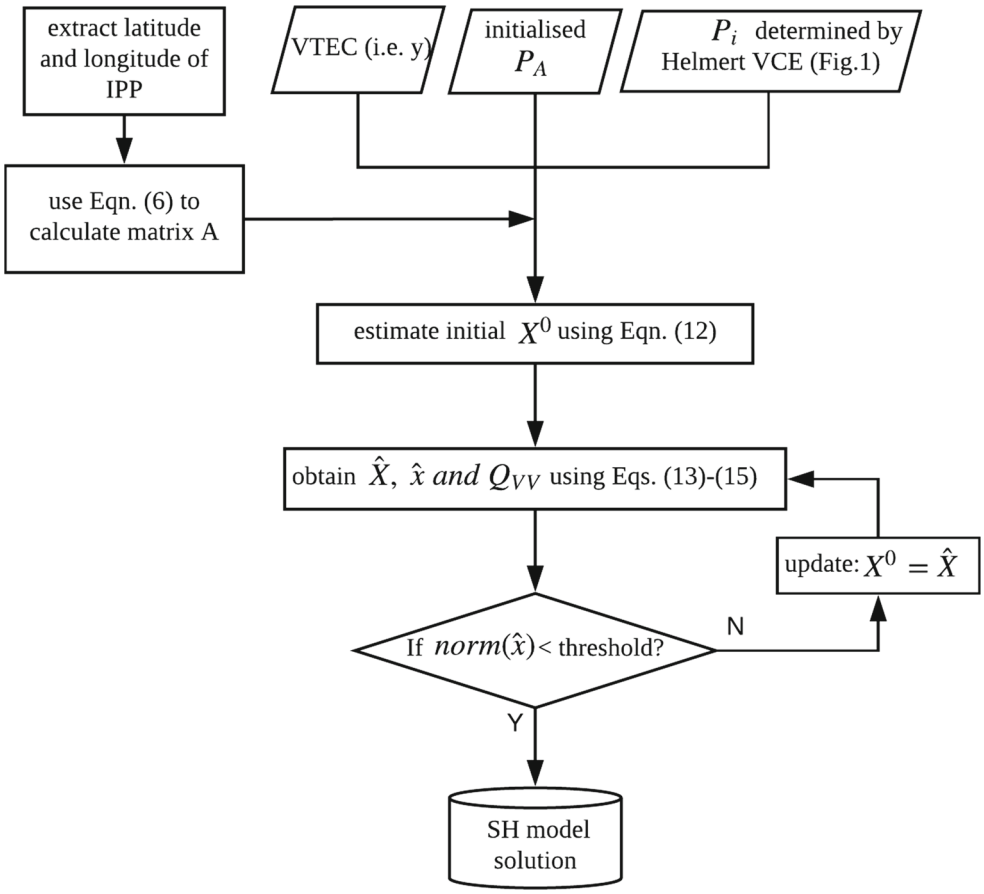

Fig. 2 Procedure for the fast-WTLS

where N and M are the number of the observations and unknown coefficients to be estimated; and the kronecker product $\otimes$ and vector operator vec() are defined in Henderson and Searle(1981) and Zehfuss (1858).

The procedure for the fast-WTLS is shown in Fig. 2.

Although the above simplified formulas are used, the fast-WTLS still needs a large computational effort. Hence the sequential adjustment method was adopted in this study because all the VTEC observations are considered independent.

It is noted that $Q_{\mathrm{vec}(\hat{G})}$ can be simplified for improving computational efficiency because it is diagonal, and the same is true for Q_{VV}. In summary, the whole procedure of the proposed method is:

1. Select VTEC data from IGS, satellite altimetry and RO databases;
2. Use the fast-WTLS approach and weights of the three data sources to solve the coefficients;
3. Apply the Helmert-VCE approach to adjust the weight of each type of the VTEC data ($\hat{P}_{\mathrm{IGS}}$, $\hat{P}_{\mathrm{RO}}$, and $\hat{P}_{\mathrm{Jason}}$). If the differences of the RMS among the three data sources are larger than the threshold (manually set), go to step (2); otherwise, go to step (4);
4. Use the current values of unknown coefficient parameters for the final solution of the VTEC model for GIM.

4 Experiments

4.1 Data selection

The datasets selected for tests were VTEC from all the 478 IGS tracking stations, COSMIC/FC-3 ionprf (level 2a, COSMIC real time data—cosmicrt) and Jason-3 IGDR data during the period of DOY 217–225, 2016. Over this period, solar and geomagnetic activity levels were mostly rather quiet. The F10.7 index varied between 80 and 100 solar flux units, and the Kp index was predominantly below 4 which constitutes quiet/stable ionospheric conditions.

The distribution of each of the three types of data on DOY 217, 2016 is shown in Fig. 3. We can see that the three data sources together cover the land and oceans globally well and the COSMIC RO data cover the polar regions where there were no Jason-3 measurements.

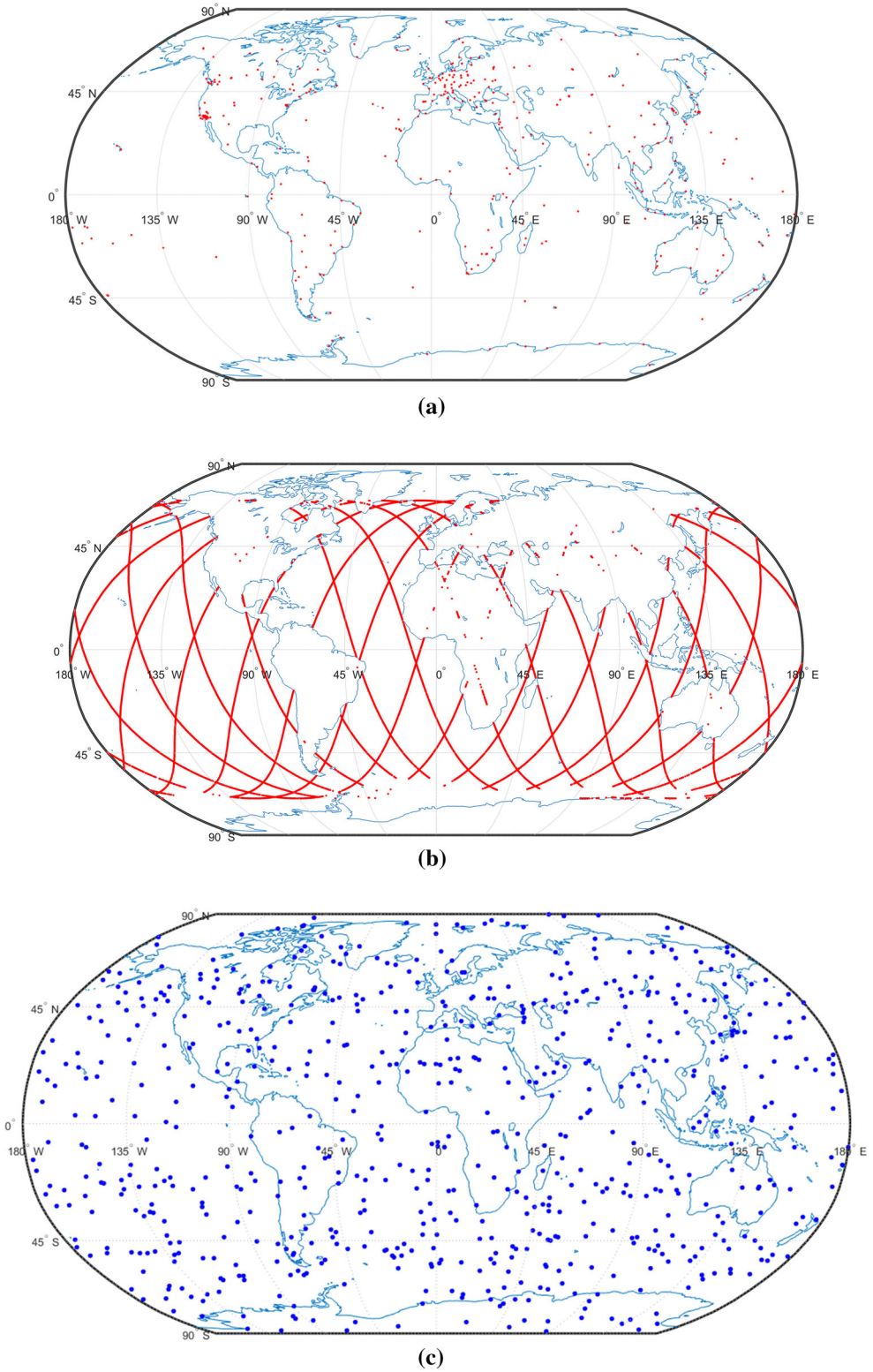

Fig. 3 Distribution and coverage of each source of data on DOY 217, 2016 **a** IGS tracking stations; **b** ocean-altimetry-satellite-derived VTECs; and **c** COSMIC ionospheric occultation events

4.2 Model performance

In order to assess the improvement of the new approach, the latest GIM developed by the GIPP of the Chinese Academy of Sciences (hereinafter called "CAS") (Li et al. 2015; Yuan et al. 2015) is used as a reference. The CAS model was based on SHPTS and validated using several data sources. This includes the ionospheric TECs retrieved from global GPS data, the GIMs released by the other Ionospheric Associate Analysis Centers (IAACs), the TOPEX/Poseidon satellite and the DORIS, etc. According to Li et al. (2015), the CAS model could achieve an accuracy of approximately 2–6 TECu over areas without GNSS observations, and its performance is similar to those of other models released by IAACs. To further validate the accuracy of the new model, out-of-sample Jason-3 measurements are also used as an external reference in this study.

4.2.1 In comparison with other models

Three schemes, named "Scheme-1", "Scheme-2" and "Scheme-3", were used to test the performance of WLS, Helmert-aided WLS and Helmert-aided WTLS models, respectively. Results of comparisons between the three schemes on DOY 224 are shown in Fig. 4.

Figure 4 reveals that, compared with the WLS, both the Helmert and WTLS approaches can significantly affect the GIM results (see yellow and blue shadings). To investigate

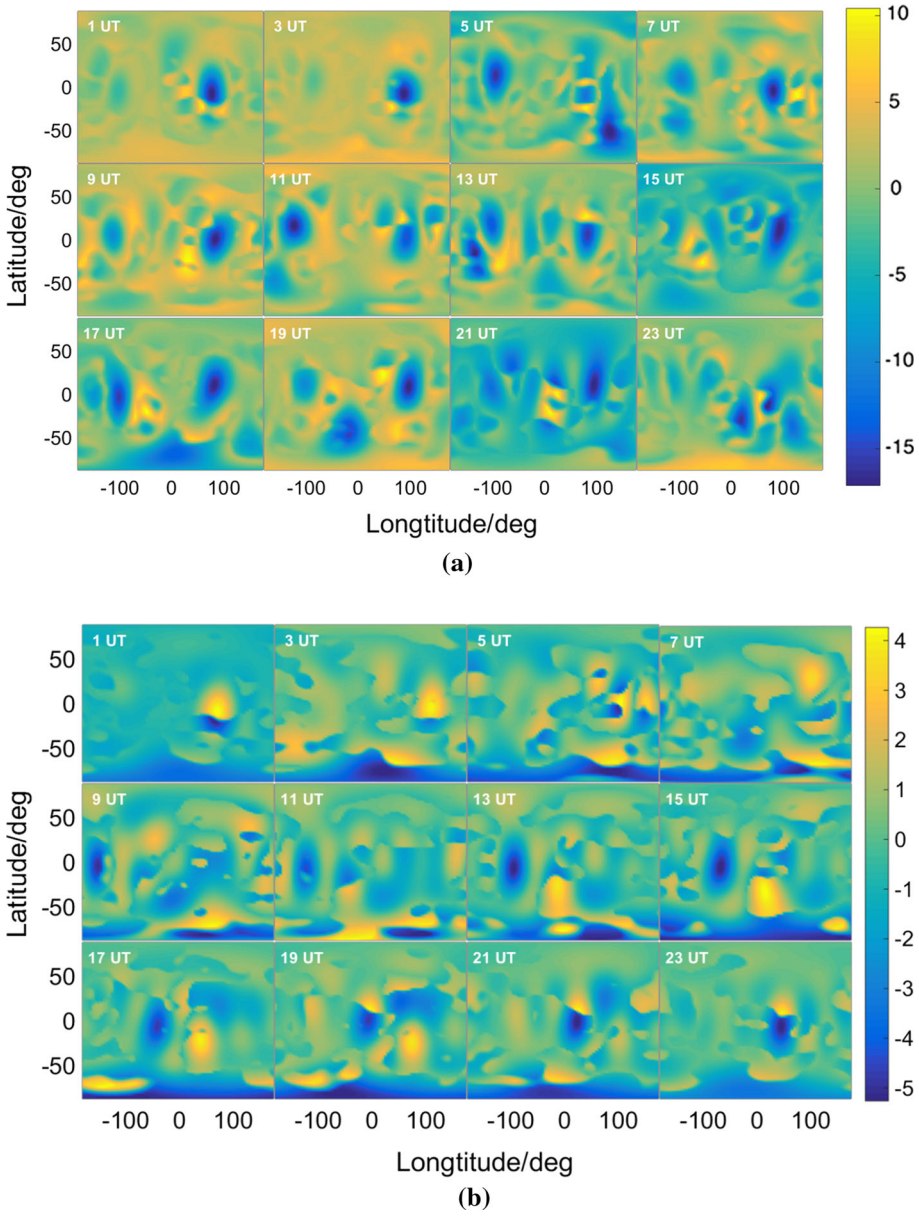

Fig. 4 Snapshots (every 2 h on DOY 224, 2016) of the global distribution of the difference (unit: TECU): **a** between the VTECs obtained from Scheme-1 and Scheme-2; and **b** between Scheme-2 and Scheme-3. The two axes are the sun-fixed geomagnetic latitude and longitude (equivalent to local time) with a resolution of 2.5° × 5°

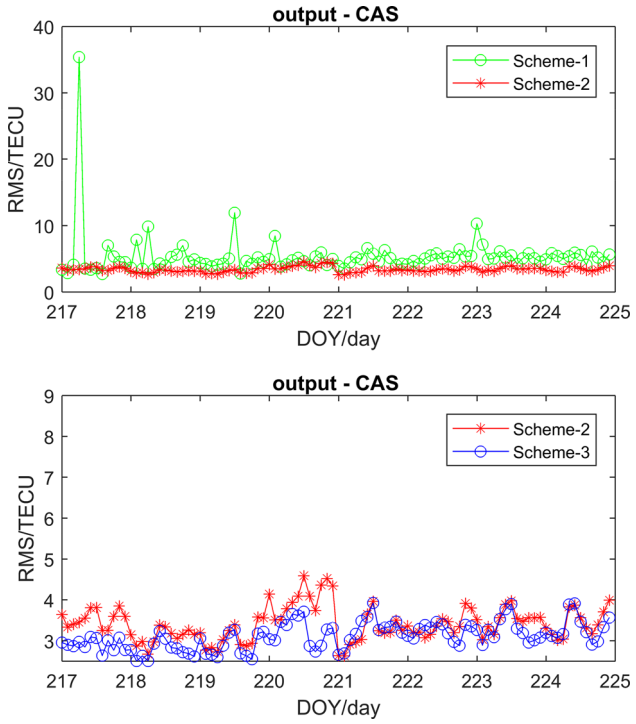

Fig. 5 Time series of the RMS (every 2 h time slot) of global grids' VTECs in the period of DOY 217–224, 2016 (the reference is CAS)

Table 1 Mean and STD of RMSs of global grids' VTECs of all 2-h time slots for each scheme shown in Fig. 5 (unit: TECU, the best performance is shown in bold)

Scheme	Reference: CAS	
	Mean	STD
1	4.98	3.42
2	3.37	0.41
3	**3.09**	**0.34**

if the proposed Helmert-WTLS approach can improve the accuracy of VTEC modelling, the aforementioned GIM provided by the GIPP of the CAS was selected to represent the near real-time VTEC model. As a result, the difference between the model and the reference was used to measure the accuracy of the VTEC SH model. Figure 5 shows the time series of the root-mean-square (RMS) of all global grids' VTECs of every 2 h in the 8-day test period. Table 1 lists the mean and standard deviation (STD) of the time series results shown in Fig. 5 for the overall accuracy of the period.

The top subfigure in Fig. 5 indicates that, generally, the results of Scheme-2 (red) are better than Scheme-1 (green) and the bottom panel shows Scheme-3 (blue) is better than Scheme-2. In addition, an anomaly from Scheme-1 is shown in the top subfigure (in the morning of DOY 224). This is likely to be caused by the inappropriate weights used for the different types of the VTEC data, especially in the case that some outliers exist. The fact that this anomaly does not exist in the results of the other two schemes implies that the proposed approach is better in outlier resistance. The outlier (large anomaly) is excluded in the calculation of the statistical results shown in the table below to avoid the statistics of the top subfigure in Fig. 5 from being distorted.

It can be seen that the last row, i.e. Scheme-3, achieved the best performance. Compared to Scheme-2, an improvement of 8% (w.r.t CAS outputs) has been achieved. Compared to Scheme-1, an improvement of 32% has been achieved.

Figure 6 shows the variations in the RMS of the above VTECs from the same time slot but different days which are extracted from Fig. 5 results. These results indicate that both Scheme-2 and Scheme-3 consistently and significantly outperformed Scheme-1 in all the 12 time slots (1–23 UT), and the majority of the Scheme-3 results outperformed Scheme-2.

4.2.2 A comparison with out-of-sample IGS and Jason-3 observations

In order to further assess the performance of the three schemes, especially over ocean regions (which is the weakness of the traditional models), out-of-sample (i.e. those samples which have not been considered in modelling, normally 15% of the whole sample set) IGS (over continents) and Jason-3 observations (over oceans) are used as the reference (i.e. ground truth) for continents and oceans to investigate the differences among three schemes.

IGS data were a traditional reference for GIM assessment, and the Jason-3 data were selected due to the following two primary considerations.

1. Both the Jason and RO measurements cover most ocean areas (as Fig. 3b), which is the essential region where performance needs to be improved. However, the number of RO measurements during the 2-h period is too few to extract enough measurements as a test dataset.
2. The VTECs from other two data sources (IGS and RO) are under the assumption of spherical symmetry (the error caused from the assumption can be mitigated by WTLS).

The results are shown in Fig. 7, where x- and y-axes denote the DOY and absolute error, respectively. Figure 7a shows that Scheme-3 (whose mean absolute error is 4.39 TECU) outperformed the Scheme-2 (5.24 TECU) and Scheme-1 (5.39 TECU), as well as CAS and CODE (6.79 and 6.87 TECU, respectively) in most occasions during this period when Jason-3 is taken as the test dataset, which reflects that the WTLS can improve the performance of the model over ocean regions. Figure 7b shows that the performances of the three schemes in reference to IGS measurements (mostly in continent regions) are all close to 2 TECU; Scheme-2 (2.05

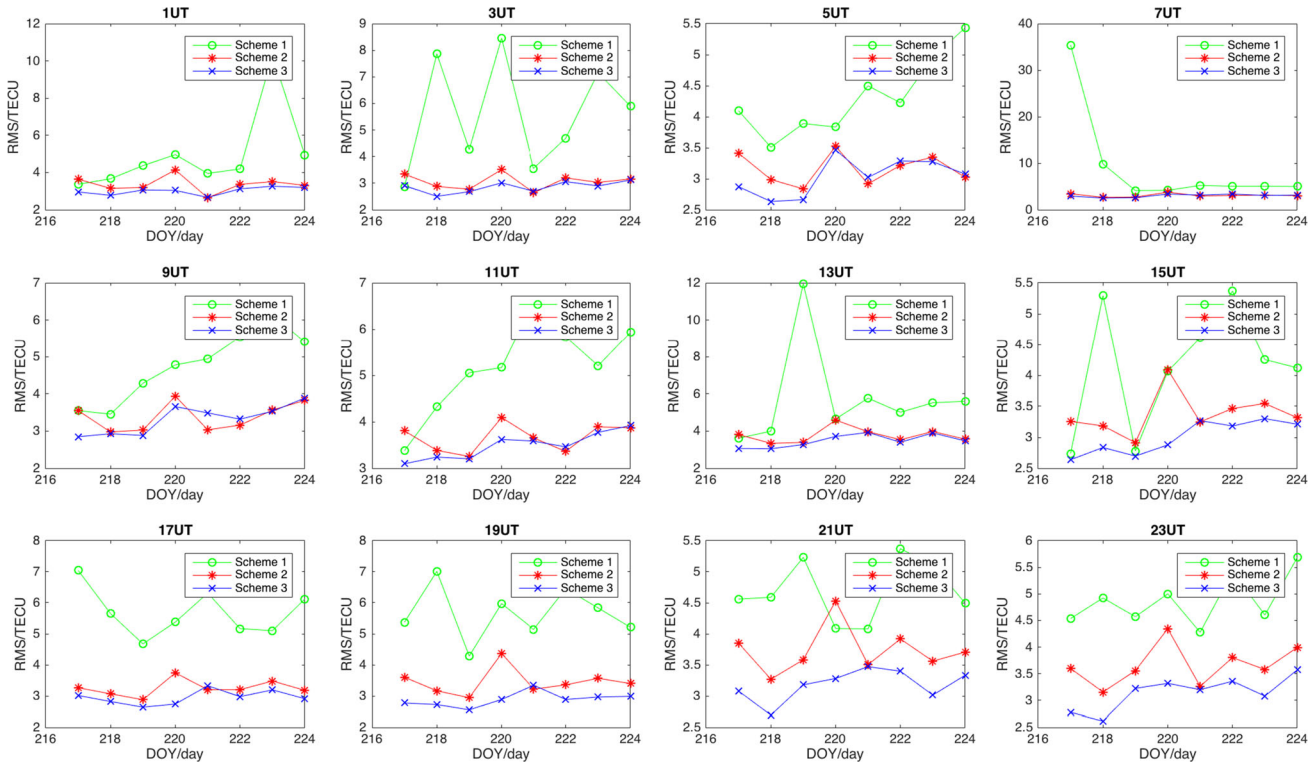

Fig. 6 RMS of all global grids' VTECs in each 2 h time slot in the period DOY 217–224, 2016 w.r.t. CAS

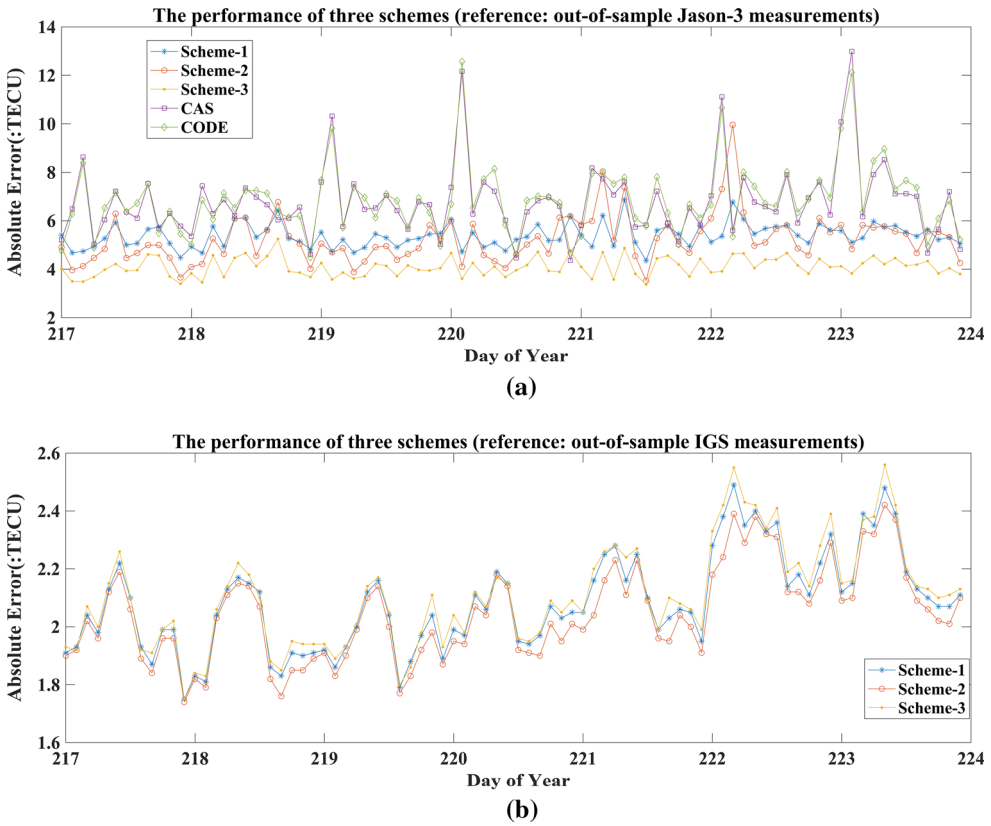

Fig. 7 The performance of three schemes and two IAAC GIMs (i.e. CAS and CODE) in comparison with out-of-sample Jason-3 measurements (shown in **a**) IGS measurements (shown in **b**) during DOY 217-225, 2016

TECU) is slightly better than Scheme-1 (2.08 TECU) and Scheme-3 (2.10 TECU).). These results are similar to current GIMs (Li et al. 2015). This result indicates that all of the proposed models can perform equally well over land due to the thorough coverage of IGS stations.

5 Conclusion

In this study, an innovative approach—Helmert-aided fast-WTLS, was proposed to enhance global VTEC modelling. Three VTEC data sources including ground-based GNSS, satellite altimetry and RO data were used to establish a global SH model for generating a GIM. Test results showed:

1. The fast-WTLS approach can improve the accuracy of the GIMs by around 5% since the uncertainty of the design matrix of the observation equations of the SH model has been taken into account;
2. The accuracy improvements were more pronounced when the GIMs provided by GIPP (i.e. CAS) was selected as the reference (roughly 8%);
3. The improvement of the proposed model over oceans was validated by using out-of-sample Jason-3 measurements as reference and about 20% improvement (mostly over the ocean) was achieved.

In the future, with the launch of the COSMIC-2 constellation on the horizon, more and more RO data will be available and the accuracy of GIMs will be improved by the use of these additional data.

Acknowledgements This work was supported by the Strategic Priority Research Program of the Chinese Academy of Sciences (No. XDA17010304) and Australian Research Council project (LP160100561). This work was also funded by the Jiangsu dual creative talents and teams programme projects awarded in 2017. We also would like to acknowledge the support of the Natural Science Foundation of China (41730109, 41674043, 41704038, 41874040), Beijing Nova programme (xx2017042), Beijing Youth Talent Support program (2017000021223ZK13), Pioneer Hundred Talents Program, National Key Research and Development Plan (2016YFB0501405) of the Chinese Academy of Sciences and Beijing Natural Science Foundation (8184092). Andong Hu acknowledges the China Scholarship Council for the provision of a scholarship for his study at the SPACE Research Centre, RMIT University. Zishen Li acknowledges the Australian Dept. of Education and Training for the provision of an Endeavour scholarship for his research at the SPACE Research Centre. We thank IGS for providing GNSS data and precise DCB values for all transmitters and receivers, UCAR/CDAAC for providing ionPrf data, and CNES and NOAA for providing Jason-3 IGDR data.

References

Alizadeh M, Schuh H, Todorova S, Schmidt M (2011) Global ionosphere maps of VTEC from GNSS, satellite altimetry, and formosat-3/COSMIC data. J Geodesy 85(12):975–987

Anthes RA et al (2008) The COSMIC/FORMOST-3 mission: early results. Am Meteorol Soc 89:313–333

Azpilicueta F, Brunini C (2009) Analysis of the bias between TOPEX and GPS vTEC determinations. J Geodesy 83(2):121–127

Bilitza D (1997) International reference ionosphere—status 1995/96. Adv Space Res 20(9):1751–1754

Bilitza D (2001) International reference ionosphere 2000. Radio Sci 36(2):261–275

Bilitza D, Reinisch BW (2008) International reference ionosphere 2007: improvements and new parameters. Adv Space Res 42(4):599–609

Bilitza D, Rawer K, Bossy L, Kutiev I, Oyama K-I, Leitinger R, Kazimirovsky E (1990) International reference ionosphere

Chen P, Yao W, Zhu X (2015) Combination of ground-and space-based data to establish a global ionospheric grid model. IEEE Trans Geosci Remote Sens 53(2):1073–1081

Ciraolo L, Azpilicueta F, Brunini C, Meza A, Radicella S (2007) Calibration errors on experimental slant total electron content (TEC) determined with GPS. J Geodesy 81(2):111–120

Dettmering D, Schmidt M, Heinkelmann R, Seitz M (2011) Combination of different space-geodetic observations for regional ionosphere modeling. J Geodesy 85(12):989–998

Dumont J, Rosmorduc V, Carrere L, Picot N, Bronner E, Couhert A, Guillot A, Desai S, Bonekamp H, Figa J (2016) Jason-3 products handbook. *Rep* SALP-MU-M-OP-16118-CN Google Scholar

Golub GH, Van Loan CF (1980) An analysis of the total least squares problem. SIAM J Numer Anal 17(6):883–893

Hajj GA, Ibanez-Meier R, Kursinski ER, Romans LJ (1994) Imaging the ionosphere with the global positioing system. Int J Imaging Syst Technol 5:174–184

Henderson HV, Searle SR (1981) The vec-permutation matrix, the vec operator and Kronecker products: a review. Linear Multilinear Algebra 9(4):271–288

Hernández-Pajares M, Juan J, Sanz J (1999) New approaches in global ionospheric determination using ground GPS data. J Atmos Solar Terr Phys 61(16):1237–1247

Hernández-Pajares M, Juan JM, Sanz J, Orus R, Garcia-Rigo A, Feltens J, Komjathy A, Schaer SC, Krankowski A (2009) The IGS VTEC maps: a reliable source of ionospheric information since 1998. J Geodesy 83(3):263–275. https://doi.org/10.1007/s00190-008-0266-1

Hernández Pajares M, Roma Dollase D, Krankowski A, García Rigo A, Orús Pérez R (2016) Comparing performances of seven different global VTEC ionospheric models in the IGS context. In: Paper presented at international GNSS service workshop (IGS 2016): Sydney, Australia: 8–12 Feb 2016, International GNSS Service (IGS)

Hochegger G, Nava B, Radicella S, Leitinger R (2000) A family of ionospheric models for different uses. Phys Chem Earth Part C Solar Terr Planet Sci 25(4):307–310

Imel DA (1994) Evaluation of the TOPEX/poseidon dual-frequency ionosphere correction. J Geophys Res Oceans 99(C12):24895–24906

Li Z, Yuan Y, Li H, Ou J, Huo X (2012) Two-step method for the determination of the differential code biases of COMPASS satellites. J Geodesy 86(11):1059–1076

Li Z, Yuan Y, Wang N, Hernandez-Pajares M, Huo X (2015) SHPTS: towards a new method for generating precise global ionospheric TEC map based on spherical harmonic and generalized trigonometric series functions. J Geodesy 89(4):331–345

Mannucci A, Wilson B, Yuan D, Ho C, Lindqwister U, Runge T (1998) A global mapping technique for GPS-derived ionospheric total electron content measurements. Radio Sci 33(3):565–582

Radicella S, Leitinger R (2001) The evolution of the DGR approach to model electron density profiles. Adv Space Res 27(1):35–40

Schaffrin B, Wieser A (2008) On weighted total least-squares adjustment for linear regression. J Geodesy 82(7):415–421

Scherliess L, Schunk RW, Sojka JJ, Thompson DC (2004) Development of a physics-based reduced state Kalman filter for the ionosphere. Radio Sci 39(1):RS1S04

Schreiner W, Rocken C, Sokolovskiy S, Syndergaard S, Hunt D (2007) Estimates of the precision of GPS radio occultation from the COSMIC/FORMOSAT-3 mission. Geophys Res Lett 34(4):L04808

Schunk RW, Scherliess L, Sojka JJ, Thompson DC, Anderson DN, Codrescu M, Minter C, Fuller-Rowell TJ, Heelis RA, Hairston M (2004) Global assimilation of ionospheric measurements (GAIM). Radio Sci 39(1):RS1S04

Shen Y, Li B, Chen Y (2011) An iterative solution of weighted total least-squares adjustment. J Geodesy 85(4):229–238

Sokolovskiy S, Rocken C (2006) Algorithms for inverting radio occultation signals in the ionosphere. University Corporation for Atmospheric Research

Todorova S, Hobiger T, Schuh H (2008) Using the global navigation satellite system and satellite altimetry for combined global ionosphere maps. Adv Space Res 42(4):727–736

Wang N, Yuan Y, Li Z, Montenbruck O, Tan B (2016) Determination of differential code biases with multi-GNSS observations. J Geodesy 90(3):209–228

Xu P, Shen Y, Fukuda Y, Liu Y (2006) Variance component estimation in linear inverse ill-posed models. J Geodesy 80(2):69–81

Yuan Y, Li Z, Wang N, Zhang B, Li H, Li M, Huo X, Ou J (2015) Monitoring the ionosphere based on the crustal movement observation network of China. Geodesy Geodyn 6(2):73–80

Zehfuss G (1858) Über eine gewisse determinante. Z Math Phys 3(1858):298–301